Photometric Asymmetry Between Clockwise and Counterclockwise Spiral Galaxies in SDSS

Lior Shamir

Lawrence Technological University, 21000 W Ten Mile Rd, Southfield, MI 48075, USA
Email: lshamir@mtu.edu

Abstract

While galaxies with clockwise and counterclockwise handedness are visually different, they are expected to be symmetric in all of their other characteristics. Previous experiments using both manual analysis and machine vision have shown that the handedness of Sloan Digital Sky Survey galaxies can be predicted with accuracy significantly higher than mere chance using its photometric data alone. However, some of these previous experiments were based on manually classified galaxies, and the results may therefore be subjected to bias originated from the human perception. This paper describes an experiment based on a set of 162,514 galaxies classified automatically to clockwise and counterclockwise spiral galaxies, showing that the source of the asymmetry in Sloan Digital Sky Survey database is not the human perception bias. The results are compared to two smaller datasets, and confirm the observation that the handedness of SDSS galaxies can be predicted by their photometry. The experiment also shows statistically significant differences in the measured magnitude of SDSS galaxies, according which galaxies with clockwise patterns are brighter than galaxies with counterclockwise patterns. The magnitude of that difference changes across RA ranges, and exhibits a strong correlation with the cosine of the right ascension.

Keywords: Galaxies: general – galaxies: photometry – galaxies: spiral

1 INTRODUCTION

While galaxies with clockwise handedness are expected to be symmetric to galaxies with counterclockwise handedness, previous experiments (Shamir 2016) have shown that clockwise galaxies imaged by Sloan Digital Sky Survey (York et al. 2000) are photometrically different from galaxies with counterclockwise patterns. The experiment was done by separating a population of spiral galaxies into clockwise and counterclockwise galaxies, and then collecting the photometric information of each galaxy from SDSS Catalog Archive Server (CAS). That was done by using the Galaxy Zoo 2 (Willett et al. 2013) galaxies classified manually as spirals, as well as with another dataset of 10 281 galaxies classified as clockwise and counterclockwise spiral galaxies in a fully automatic process, and without human intervention.

Then, supervised machine learning was trained using these photometric data such that the label of each class was the handedness. Experimental results show that by using the photometric information the handedness of the galaxy (clockwise or counterclockwise) can be predicted in accuracy of ∼64%, which is much higher than random guessing accuracy of 50% ($P<10^{-5}$). The experiment using the dataset of galaxies that

were annotated in a fully automatic process provided a comparable handedness prediction accuracy of ∼65%. The analysis also revealed that several different photometric measurements such as the SDSS 'Stokes U' parameter exhibit a statistically significant difference between clockwise and counterclockwise galaxies (Shamir 2016).

Other observations related to handedness asymmetry measured the number of clockwise and counterclockwise galaxies, showing evidence of asymmetry between the number of clockwise and counterclockwise galaxies. Land et al. (2008) used a large dataset of galaxies annotated by crowdsourcing, showing that after correcting for the substantial human bias the number of galaxies with clockwise handedness was higher than the number of counterclockwise galaxies, but the difference was not statistically significant (Land et al. 2008). A more recent analysis using 13 440 automatically classified galaxies (Shamir 2016) showed a higher number of galaxies with clockwise handedness compared to galaxies with counterclockwise handedness, which is also in agreement with the higher number of Galaxy Zoo (Lintott et al. 2011) clockwise galaxies observed in Shamir (2012). On the other hand, the dataset of 10 281 galaxies used in Shamir (2016) showed no statistically significant preference (Shamir 2016).

Since most of these studies were done by using manual classification of the galaxies, a possible explanation is that the asymmetry is driven by a bias in the human perception. This paper describes an experiment that uses data annotated in a fully automatic process, and with no human intervention that can induce bias. Since the dataset is far larger than previous datasets used for that purpose, it can also be used to show statistically significant differences between measurements of galaxies with clockwise patterns and galaxies with counterclockwise patterns.

2 DATA

The galaxies used in the experiment were galaxies classified as spiral galaxies in the catalogue of broad morphology of ∼3 000 000 SDSS Data Release 8 galaxies (Kuminski & Shamir 2016), which was generated automatically by applying the Wndchrm image classifier (Shamir et al. 2008, 2013) to the galaxy images (Shamir 2009; Kuminski et al. 2014). The initial set of ∼3 000 000 galaxies was selected such that all galaxies had a Petrosian radius (measured on the *r* band) of at least 5.5 arcsec, the Petrosian radius error was less than 5 arcsec, and the flags were selected such that none of the objects was identified as 'bad sky', 'bad radial', 'too large', too close the edge of the frame, or had more than one peak or Petrosian radius (Kuminski & Shamir 2016). These constraints provided a set of galaxies with identifiable morphology, allowing their separation into spiral and elliptical galaxies. That was done by applying an automatic classifier that can analyse galaxy images and annotate them with their broad morphological types (Shamir 2009; Kuminski et al. 2014). Each galaxy was assigned with its broad morphological type of early or late type, but also with the certainty value within the interval (0,1) that the classification is correct. A certainty value close to 0.5 means that the certainty of the classification is nearly random, while a certainty value close to 1 indicates that there is a very low chance that the annotation is incorrect. A detailed description of the catalogue is available in Kuminski & Shamir (2016).

Galaxies that were classified as spiral galaxies with certainty higher than 0.54 were used in the experiment, providing a dataset of 740 908 spiral galaxies (Kuminski & Shamir 2016). To assess the consistency of the galaxy catalogue compared to manual annotation of the galaxies, the galaxies were compared to the manual annotation of *Galaxy Zoo*. That was done by identifying all galaxies that are included in the catalogue and were also classified by *Galaxy Zoo* as debiased 'superclean', and comparing the morphological annotation of the catalogue to the morphological annotation of the superclean *Galaxy Zoo*. Statistical analysis of the 45 377 galaxies included in the catalogue and were also classified by *Galaxy Zoo* as debiased 'superclean' showed that in ∼98% of the cases, these galaxies are also identified as spiral by the debiased 'supercleasn' *Galaxy Zoo* dataset (Kuminski & Shamir 2016), showing that the set of spiral galaxies is reasonably accurate for the purpose of identifying spiral galaxies in SDSS.

Similarly to Shamir (2016), the spiral galaxies were separated by their handedness to clockwise and counterclockwise galaxies using the *Ganalyzer* algorithm (Shamir 2011a, 2011b), which converts each galaxy image to its radial intensity plot, and then applies automatic peak detection to find and group the peaks along the horizontal line of the radial intensity plot (Shamir 2011b). Since the galaxy arms are brighter than non-arm pixels at the same radial distance, the peaks are expected to identify the arms. Linear regression is applied across the vertical lines of the radial intensity plot for each group of peaks, and the sign of the slopes reflect the direction of the arm, therefore determining the handedness of the galaxy. The algorithm is described in details and numerous examples in Shamir (2011b), Hoehn & Shamir (2014), Shamir (2012), and the process of galaxy classification is described in Shamir (2016).

The process of the separation of the galaxies to clockwise and counterclockwise described above provided a dataset of 82 244 galaxies with clockwise handedness and 80 272 galaxies with counterclockwise handedness. The remaining galaxies did not have a clear handedness determined by Ganalyzer, and were therefore excluded from the experiment.

As the results show, the number of galaxies with clockwise patterns is higher than the number of galaxies with counterclockwise patterns. Assuming random 0.5 probability of the galaxy to have each of the two possible patterns, the probability to have such separation by chance can be computed using cumulative binomial distribution, such that the number of tests is 162 516 and the probability of success is 0.5. The probability to have 82 244 or more successes is $P \simeq 5 \times 10^{-7}$.

The higher number of clockwise galaxies is aligned with the ratio between clockwise and counterclockwise galaxies in datasets of manually classified spiral galaxies (Shamir 2016, 2012; Hoehn & Shamir 2014). Other experiments using automatic (Shamir 2016) and manually (Land et al. 2008) classified galaxies showed a higher number of galaxies with clockwise handedness, although the difference was not statistically significant.

After the galaxies were classified, 400 random galaxies classified by Ganalyzer as clockwise and 400 random galaxies classified by Ganalyzer as counterclockwise were examined manually to test the consistency of the dataset. Twenty four galaxies classified as clockwise had no clear identifiable handedness, as well as 21 galaxies that were classified by Ganalyzer as counterclockwise. However, none of the galaxies that were examined was clearly misclassified.

Figure 1 shows the distribution of the *r* magnitude, Petrosian radius measured in the *r* band, and the redshift of the galaxies classified by Ganalyzer as clockwise, counterclockwise, and galaxies that could not be classified to any of these classes and remained unclassified. The vast majority of the galaxies do not have spectra, and therefore just 10 281 galaxies that had redshift information could be used.

As the figure shows, while galaxies with higher *r* magnitude tend to be classified less frequently into clockwise or counterclockwise galaxies, the distribution of the galaxies
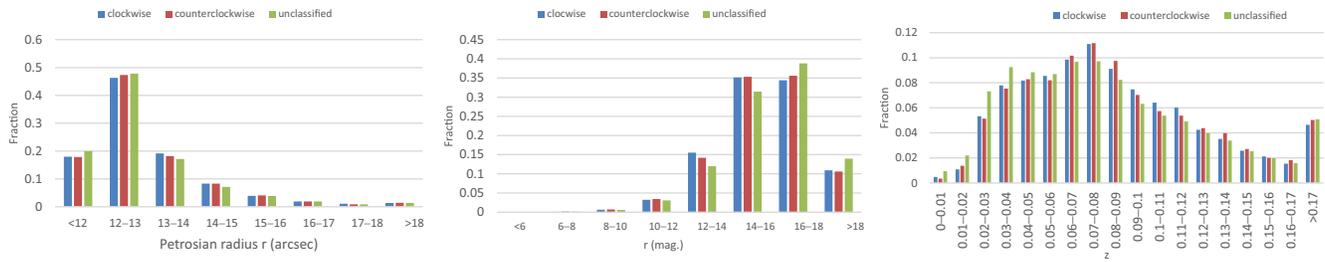
Figure 1. Distribution of the *r* magnitude, Petrosian radius measured in the *r* band, and the distribution of redshift. The distribution of magnitude and radius was measured with the entire dataset, while the distribution of the redshift is among a subset of 10 281 galaxies with spectra.

that could not be classified by *Ganalyzer* is largely aligned with the distribution of the galaxies that were classified as clockwise or counterclockwise.

3 ANALYSIS AND RESULTS

Since galaxies are described by multiple measurements rather than a single parameter (Brosche 1973; Djorgovski & Davis 1987), all of the 509 photometric variables from SDSS Data Release 8 (Aihara et al. 2011) PhotoObjAll table were used for each galaxy in the dataset. As in Shamir (2016), the galaxies were classified automatically by four different supervised machine learning algorithms: Random Forest (Breiman 2001), Decision Table (Kohavi 1995), Ensembles of Balanced Nested Dichotomies (Dong, Frank, & Kramer 2005), and Bagging (Breiman 1996). The features of each galaxy were the PhotoObjAll photometric variables, and the class label of each galaxy was its handedness. That is, the purpose of the supervised machine learning was to identify the handedness of a galaxy based on its DR8 photometric variables. Assuming no link between the photometry of the galaxy and its handedness, the prediction accuracy is expected to be equal to random guessing, which would provide 50% classification accuracy.

Some SDSS galaxies have photometric values such as -9999, which are actually flags and not actual photometric measurements. Since the purpose of the experiment is to analyse the photometry of galaxies, galaxies with photometric values such as -9999 were ignored.

The machine learning was done using the open source Waikato Environment for Knowledge Analysis (WEKA) software (Frank et al. 2004; Hall et al. 2009). The experiments were performed such that 80% of the galaxies were used for training, and the remaining 20% were used for testing the ability of the classifier to correctly identify the handedness of the galaxy based on its photometric variables. The classification accuracy was determined by the number of galaxies which their handedness was predicted correctly, divided by the total number of galaxies. Additionally, the same experiments were repeated such that random handedness was assigned to each galaxy. The results are displayed in Figure 2.

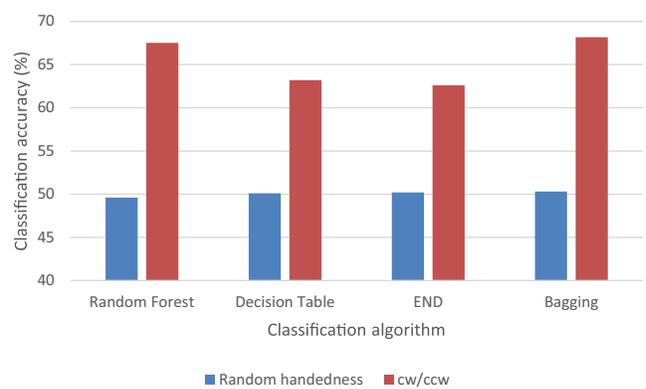The graph clearly shows that the photometric variables computed by SDSS contain information related to the hand-

Figure 2. Prediction accuracy of the handedness using the photometric information. The graph also shows the prediction accuracy when the handedness of each galaxy was replaced with a random handedness.

edness, and that the handedness of the galaxy can be predicted by using its SDSS photometric variables. When a random handedness is assigned to each galaxy, the classification accuracy drops to the $\sim$50% mere chance accuracy. Differences in the classification accuracy achieved by each of the machine learning algorithms are expected, as not all machine learning algorithms are equally powerful, and different algorithms may perform differently on different datasets.

To achieve classification accuracy of 68.15% as was achieved using the Bagging classification method, 22 151 galaxies should be classified correctly out of the total of 32 503 galaxies used for testing. The probability for 22 151 galaxies to be classified accurately by chance can be computed using cumulative binomial probability such that the number of tests is 32 503, the minimum number of successes is 22 151, and the probability of success in each test is 0.5. The probability for 22 151 or more successes is extremely low ($P < 10^{-5}$). These results are in agreement with previous studies using manually classified data or smaller sets of automatically classified galaxies, in which comparable accuracy of $\sim$65% was observed for the automatic prediction of the handedness of the galaxy (Shamir 2016).

The prediction of the handedness was done using all variables in SDSS DR8 PhotoObjAll table. To identify variables that exhibit statistically significant difference between clockwise and counterclockwise galaxies, all variables were

compared using an unpaired *t*-test. In the absence of an hypothesis regarding the direction of the expected difference, the two-tailed *P* values were used.

When a large set of tests are performed, the probability that one of these tests provides statistically significant difference increases when the total number of tests gets higher. To avoid false positives, the Bonferroni correction (Goeman & Solari 2014) was applied to the *t*-test *P* values, so that the *P* value of each hypothesis is corrected for the total number of hypotheses analysed in the experiment. Table 1 shows the variables that exhibit a Bonferroni-corrected statistical significance of *P* < 0.05 for the difference between the values measured from clockwise galaxies and the values measured from counterclockwise galaxies.

The table shows that several different variables show a Bonferroni-corrected statistically significant difference between clockwise and counterclockwise galaxies. Some of these variables are the DeVaucouleurs fit position angle (de-VPhi) variables computed from the *u*, *g*, *r*, *i*, and *z* bands, as well as the variables from the exponential fit position angle (expPhi) computed in the same bands. All of these variables show that the position angle measured for clockwise galaxies is, on average, smaller than the position angle measured for the galaxies that have counterclockwise patterns. The observation that the position angle is higher when measured on counterclockwise galaxies is in agreement with the analysis performed in Shamir (2016), indicating that the source of the asymmetry observed in Shamir (2016) is not the human bias, but could be attributed to errors in the measurements performed by SDSS photometry pipeline. The SDSS 'Stokes U' parameter measured in the *r* band (*u_r*) also shows statistically significant difference. That observation also agrees with the differences in the 'Stokes U' measured in the manually classified galaxies (Shamir 2016), although in this experiment, statistically significant differences were only observed in the *r* band. The SDSS 'Stokes U' parameter in SDSS is defined by $U = \frac{a-b}{a+b} \sin(2\phi)$, where *b* is the galaxy's minor axis, *a* is the major axis, and ϕ is the position angle (Abazajian et al. 2009). Since 'Stokes U' is a function of the position angle, asymmetry in the measurement of the position angle could lead to differences in the measurement of the SDSS 'Stokes U'.

The other photometric variables computed by SDSS pipeline that exhibit a statistically significant difference between clockwise and counterclockwise galaxies are related to the magnitude, showing that clockwise galaxies imaged by SDSS are brighter than counterclockwise galaxies. The PSF magnitude (psfMag) measurements on band *g* and *z* exhibit a statistically significant difference between clockwise and counterclockwise spiral galaxies, showing that clockwise galaxies observed through SDSS are brighter than counterclockwise galaxies. The same is observed by the comparison of the 3 arcsec fiber magnitude (fiberMag) and 2 arcsec fiber magnitude (fiber2Mag) measured in the *g*, *r*, *i*, and *z* bands measured by SDSS photometric pipeline. The de Vaucouleurs magnitude fit (deVMag) and exponential magnitude fit (exp-

Mag) measured on the *z* band, and the Petrosian magnitude measured on the *g* and *i* band also show that clockwise galaxies are brighter than counterclockwise galaxies. The PSF flux (psfFlux) and the 3 arcsec fiber flux (fiberFlux) are higher for counterclockwise galaxies, with statistically significant difference observed in the *g*, *r*, *i*, and *z* bands. The inverse variance of the Petrosian flux (petroFluxIvar) shows that the measurement of counterclockwise galaxies is less noisy compared to clockwise galaxies.

The model magnitude computed by SDSS pipeline also shows that in SDSS database, galaxies with clockwise handedness are brighter than galaxies with counterclockwise handedness, as shown in Table 2. Although the Bonferroni-corrected *P* values of these differences are not statistically significant, they are aligned with the magnitude differences shown in Table 1.

The SDSS ratio between the major and minor axes measured using the exponential model fit (expAB) and the De-Vaucouleurs model fit (DeVAB) measured in bands *g*, *r*, and *i* are significantly different between clockwise galaxies and counterclockwise galaxies in SDSS database, showing that according to the SDSS photometric pipeline, counterclockwise galaxies tend to be more round than clockwise galaxies.

Given the high number of variables being tested, after the Bonferroni correction, the *P* values of some of the differences might not be statistically significant. However, the differences between clockwise and counterclockwise galaxies are still in agreement with the statistically significant variables specified in Table 1. For instance, Table 3 shows the mean, standard error of the mean, and *P* values of the psfMag on the *i* and *r* bands, as well as the fiberFlux, fiberFluxVar, and fiber2FluxIvar measured on the *z* band.

As the table shows, the Bonferroni-corrected *P* values of these variables do not show statistical significance, but the differences between the values measured from clockwise and counterclockwise galaxies are in agreement with the difference measured on the other bands. Therefore, while the difference in psfMag of SDSS photometric pipeline measured in the *r* band does not exhibit strong Bonferroni-corrected statistical significance as shown by the psfMag measured in the *g* band, the values measured in the *r* and *i* bands are clearly not in conflict with the psfMag measured on the other bands.

3.1. Comparison with previous results

The results shown in Table 1 were compared to previous experiments using galaxies that were annotated as spiral by Galaxy Zoo 2 (Shamir 2016). Among the variables in Table 1 showing asymmetry between clockwise and counterclockwise galaxies, just the 'Stokes U' parameter measured in the *r* band also showed statistical significance in the Galaxy Zoo 2 annotated galaxies (Shamir 2016). That can be explained by the far smaller size of the set of Galaxy Zoo 2 spiral galaxies, not allowing the strong statistical significance of the difference that can be shown when the number of galaxies is high. Another reason can be the distribution of the Galaxy Zoo 2

Table 1. Variables with Bonferroni-corrected statistically significant difference between clockwise and counterclockwise galaxies.

Variable	Mean clockwise	Mean counterclockwise	t-test P	Bonferroni-corrected t-test P
psfMag_g	19.73 ± 0.003	19.75 ± 0.003	0.00003	0.01
psfMag_z	18.39 ± 0.003	18.4 ± 0.003	0.00006	0.03
fiberMag_g	19.65 ± 0.003	19.67 ± 0.003	0.00003	0.01
fiberMag_r	18.89 ± 0.003	18.91 ± 0.003	0.00005	0.02
fiberMag_i	18.48 ± 0.003	18.5 ± 0.003	0.00004	0.02
fiberMag_z	18.20 ± 0.003	18.22 ± 0.003	0.00004	0.02
fiber2Mag_g	20.39 ± 0.003	20.4 ± 0.003	0.00005	0.02
fiber2Mag_r	19.62 ± 0.003	19.64 ± 0.003	0.00007	0.03
fiber2Mag_i	19.21 ± 0.003	19.23 ± 0.003	0.00007	0.03
fiber2Mag_z	18.91 ± 0.003	18.94 ± 0.003	0.00006	0.03
petroMag_g	17.53 ± 0.004	17.55 ± 0.003	0.00008	0.04
petroMag_i	16.54 ± 0.003	16.56 ± 0.003	0.00005	0.02
deVMag_z	15.89 ± 0.004	15.91 ± 0.004	0.0001	0.04
expMag_z	16.39 ± 0.004	16.41 ± 0.004	0.00006	0.03
psfFlux_g	18.39 ± 0.11	17.86 ± 0.08	0.00006	0.03
psfFlux_r	34.47 ± 0.17	33.5 ± 0.15	0.00005	0.021
psfFlux_i	49.23 ± 0.26	47.77 ± 0.22	0.00002	0.007
psfFlux_z	67.68 ± 0.35	65.51 ± 0.31	$<10^{-5}$	0.001
fiberFlux_g	18.85 ± 0.09	18.39 ± 0.07	0.00005	0.02
fiberFlux_r	38.27 ± 0.16	37.34 ± 0.16	0.00004	0.02
fiberFlux_i	56.5 ± 0.24	55.1 ± 0.23	0.00003	0.01
fiberFluxIvar_g	34.82 ± 0.06	35.26 ± 0.06	$<10^{-5}$	0.0001
fiberFluxIvar_r	14.16 ± 0.02	14.38 ± 0.03	$<10^{-5}$	$<10^{-5}$
fiberFluxIvar_i	6.42 ± 0.01	6.5 ± 0.01	$<10^{-5}$	0.0002
fiber2Flux_g	9.67 ± 0.05	9.42 ± 0.04	0.00006	0.03
fiber2Flux_r	19.85 ± 0.08	19.34 ± 0.08	0.00003	0.01
fiber2Flux_i	29.46 ± 0.13	28.69 ± 0.12	0.00002	0.01
fiber2Flux_z	39.51 ± 0.18	38.45 ± 0.19	0.00007	0.03
fiber2FluxIvar_g	74.99 ± 0.14	75.96 ± 0.14	$<10^{-5}$	0.0003
fiber2FluxIvar_r	30.6 ± 0.056	31.1 ± 0.06	$<10^{-5}$	$<10^{-5}$
fiber2FluxIvar_i	14.02 ± 0.03	14.19 ± 0.03	$<10^{-5}$	0.0006
petroFluxIvar_u	0.138 ± 0.0003	0.14 ± 0.0003	0.00003	0.01
petroFluxIvar_g	0.58 ± 0.0014	0.59 ± 0.001	$<10^{-5}$	$<10^{-5}$
petroFluxIvar_r	0.26 ± 0.0007	0.27 ± 0.0007	$<10^{-5}$	$<10^{-5}$
petroFluxIvar_i	0.09 ± 0.0002	0.092 ± 0.0002	$<10^{-5}$	0.0001
petroFluxIvar_z	0.0071 ± 0.00002	0.0073 ± 0.00002	0.00002	0.01
deVAB_g	0.527 ± 0.001	0.532 ± 0.001	$<10^{-5}$	0.0001
deVAB_r	0.536 ± 0.001	0.541 ± 0.001	$<10^{-5}$	0.0002
deVAB_i	0.538 ± 0.001	0.542 ± 0.001	$<10^{-5}$	0.001
expAB_g	0.547 ± 0.001	0.551 ± 0.001	$<10^{-5}$	0.0001
expAB_r	0.553 ± 0.001	0.558 ± 0.001	$<10^{-5}$	0.0002
expAB_i	0.553 ± 0.001	0.557 ± 0.001	$<10^{-5}$	0.001
deVPhi_u	91.15 ± 0.2	88.64 ± 0.2	$<10^{-5}$	$<10^{-5}$
deVPhi_g	91.13 ± 0.2	87.58 ± 0.2	$<10^{-5}$	$<10^{-5}$
deVPhi_r	91.55 ± 0.2	88.15 ± 0.2	$<10^{-5}$	$<10^{-5}$
deVPhi_i	91.4 ± 0.2	88.22 ± 0.2	$<10^{-5}$	$<10^{-5}$
deVPhi_z	91.1 ± 0.2	88.44 ± 0.2	$<10^{-5}$	$<10^{-5}$
expPhi_u	91.06 ± 0.2	88.53 ± 0.2	$<10^{-5}$	$<10^{-5}$
expPhi_g	91.25 ± 0.2	87.44 ± 0.2	$<10^{-5}$	$<10^{-5}$
expPhi_r	91.49 ± 0.2	87.87 ± 0.2	$<10^{-5}$	$<10^{-5}$
expPhi_i	91.38 ± 0.2	87.94 ± 0.2	$<10^{-5}$	$<10^{-5}$
expPhi_z	91.01 ± 0.2	88.24 ± 0.2	$<10^{-5}$	$<10^{-5}$
u_r	-0.002 ± 0.0005	0.001 ± 0.0005	0.00002	0.01

galaxies used in the experiment. For instance, the Galaxy Zoo 2 galaxies that were used in that experiment were all in the RA range of $(90°, 270°)$, while the galaxies used in this study had no RA restriction. Also, the fact that the Galaxy Zoo galaxies were selected manually can introduce a bias driven by the human perception of the galaxies.

In addition to the Galaxy Zoo 2 galaxies, a previous experiment was also performed with a set of 10 281 automatically

Table 2. The mean, standard error of the mean, and *t*-test difference between model magnitude variables in clockwise and counterclockwise galaxies.

Variable	Mean clockwise	Mean counterclockwise	*t*-test *P*	Bonferroni-corrected *t*-test *P*
u	18.93 ± 0.004	18.95 ± 0.004	0.01	1
g	17.51 ± 0.004	17.53 ± 0.004	0.0003	0.16
r	16.82 ± 0.004	16.84 ± 0.004	0.002	1
i	16.45 ± 0.004	16.47 ± 0.004	0.0005	0.25
z	16.20 ± 0.004	16.22 ± 0.004	0.0004	0.2

Table 3. Variables that their Bonferroni-corrected *t*-test is not statistically significant, but exhibit statistically significant *t*-test when measured in other bands.

Variable	Mean clockwise	Mean counterclockwise	*t*-test *P*	Bonferroni-corrected *t*-test *P*
$psfMag\_r$	19.07 ± 0.003	19.08 ± 0.003	0.0004	0.21
$psfMag\_i$	18.71 ± 0.003	18.72 ± 0.003	0.0001	0.07
$fiberFlux\_z$	75.3 ± 0.34	73.4 ± 0.38	0.0002	0.1
$fiber2FluxIvar\_z$	1.25 ± 0.002	1.26 ± 0.002	0.006	1
$fiberFluxIvar\_z$	0.56 ± 0.001	0.57 ± 0.001	0.002	1

classified galaxies (Shamir 2016), showing that the handedness of the galaxy can be predicted by patterns of the photometric variables, but none of the single variables exhibited a Bonferroni-corrected statistical significance.

While these datasets are much smaller and therefore less likely to identify variables with a statistically significant difference between clockwise and counterclockwise galaxies, if the asymmetry is consistent across these datasets the direction of the differences between the means should be in aligned. That is, if in one dataset the mean measured in clockwise galaxies is greater than the mean measured in the counterclockwise galaxies, it is expected that the mean will be also greater among clockwise galaxies in the other datasets. Therefore, if two datasets agrees, the sign of the difference between the means of clockwise and counterclockwise galaxies should be the same in both datasets. Table 4 shows the differences between the means of clockwise and counterclockwise galaxies of the different variables. The datasets are the large dataset described in Section 2, the Galaxy Zoo 2 galaxies described in Shamir (2016), and the automatically classified galaxies described in Shamir (2016). The 'Stokes U' parameter is statistically significant in both datasets and was therefore not compared.

As the table shows, the differences between the means measured in clockwise and counterclockwise galaxies in the dataset described in Section 2 is in full agreement with the dataset of automatically classified galaxies used in Shamir (2016). In both datasets, if the mean measured on clockwise galaxies is greater than the mean measured on counterclockwise galaxies in the dataset described in Section 2, it is also greater in the dataset of the automatically classified galaxies described in Shamir (2016).

The same agreement can also be observed between the dataset described in Section 2 and the Galaxy Zoo 2 galaxies (Shamir 2016) for the position angle variables (expPhi and devPhi) measured on the different bands, as well as the deVAB and expAB variables. A clear disagreement between the dataset described in Section 2 and the Galaxy Zoo 2 galaxies is the variables related to magnitude. In the dataset described in Section 2, the magnitude of counterclockwise galaxies is higher than the magnitude of clockwise galaxies, while in the Galaxy Zoo galaxies, the magnitude of the clockwise galaxies is higher. The difference is consistent across all measurements related to the magnitude.

The disagreement between the two datasets can be explained by the fact that the Galaxy Zoo 2 galaxies are all within the RA range of (90°, 270°). As will be discussed in the next section and shown in Figure 3, in that specific RA range, the clockwise galaxies have a higher magnitude than counterclockwise galaxies also in the dataset described in Section 2, showing a full agreement between all datasets.

3.2. Results using Mpa-Jhu variables

In addition to the photometric variables in the PhotoObjAll table of SDSS, another experiment compared the variables proposed by the MPA-JHU group (Brinchmann et al. 2004), reflecting galaxy properties such as stellar mass, nebular oxygen abundance, and star-formation rate. All 193 variables from the galSpecExtra table of SDSS DR8 were used in the same fashion the PhotoObjAll variables were analysed. Since the variables are dependent on spectra, just 12 668 clockwise galaxies and 12 783 counterclockwise galaxies could be used. Table 5 shows the mean, standard error, and *t*-test

Table 4. The difference between the mean of different variables measured in clockwise galaxies and the mean measured in counterclockwise galaxies. The datasets are the dataset described in Section 2, the Galaxy Zoo 2 galaxies (Shamir 2016), and the dataset of automatically classified galaxies described in Shamir (2016).

Variable	Difference (this dataset)	Difference (Galaxy Zoo 2)	Difference (Automatic)
deVPhi_u	2.51	0.53	1.17
deVPhi_g	3.55	1.29	1.61
deVPhi_r	3.4	1.15	1.27
deVPhi_i	3.19	1.07	0.53
deVPhi_z	2.64	1.35	0.19
expPhi_u	2.53	0.75	1.34
expPhi_g	3.81	1.08	2.56
expPhi_r	3.62	1.39	1.73
expPhi_i	3.45	1.08	1.41
expPhi_z	2.77	0.95	0.91
psfMag_g	− 0.01	0.02	− 0.01
psfMag_z	-0.02	0.02	− 0.01
fiberMag_g	− 0.01	0.03	-0.01
fiberMag_r	− 0.01	0.03	− 0.01
fiberMag_i	− 0.02	0.03	− 0.01
fiberMag_z	− 0.02	0.03	− 0.01
fiber2Mag_g	− 0.01	0.03	− 0.01
fiber2Mag_r	− 0.01	0.03	− 0.01
fiber2Mag_i	− 0.02	0.03	− 0.01
fiber2Mag_z	− 0.02	0.03	− 0.005
petroMag_g	− 0.02	0.03	− 0.003
petroMag_i	− 0.02	0.04	− 0.003
deVMag_z	− 0.02	0.05	− 0.003
expMag_z	− 0.02	0.05	− 0.004
deVAB_g	− 0.005	− 0.005	− 0.002
deVAB_r	− 0.005	− 0.004	− 0.002
deVAB_i	− 0.005	− 0.005	− 0.003
expAB_g	− 0.005	− 0.005	− 0.002
expAB_r	− 0.005	− 0.004	− 0.001
expAB_i	− 0.005	− 0.005	− 0.001

of the variables that exhibited the highest statistical significance of the difference between the values measured from clockwise galaxies and the values measured from counterclockwise galaxies.

Unlike the PhotoObjAll variables, none of the MPA-JHU variables showed a Bonferonni-corrected statistical significance. However, the number of galaxies that has MPA-JHU variables is much lower than the galaxies that have photometric information. The variables that showed the highest difference between clockwise and counterclockwise galaxies are the sn1 and sn2 variables, which are the $(\frac{S}{N})^2$ when g, r, and i are 20.2, 20.25, and 19.9, respectively, and measured in both spectrographs. Other variables that showed relatively higher difference are the fracNSigma_X variables, which are the fraction of pixels more than X sigma relative to best-fit. The χ^2 of the velocity dispersion fit (velDispChi2) and the coefficients for templates 5 and 6 fit (theta_5 and theta_6) were also among the variables that showed the highest difference, but were not statistically significant even without applying a Bonferroni correction.
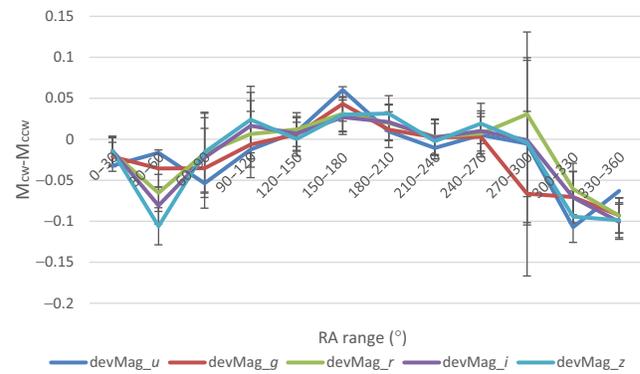
Figure 3. Differences between the de Vaucouleurs magnitude of clockwise galaxies and the de Vaucouleurs magnitude of counterclockwise galaxies in different RA ranges in the *u*, *g*, *r*, *i*, and *z* bands.

4 DISCUSSION

The handedness is a noticeable morphological characteristic of a spiral galaxy. Since the handedness is dependent on the location of the observer, spiral galaxies with clockwise patterns are expected to be fully symmetric to spiral galaxies with counterclockwise handedness. The results described here clearly show that in SDSS database, the handedness of a spiral galaxy can be predicted by the values of variables measured by SDSS photometric pipeline, showing a link between the handedness of the galaxy and its photometry.

Previous studies have shown that the human perception might not be a fully consistent tool to classify galaxies, especially when identifying the galaxy handedness (Land et al. 2008). The results of this experiment are shown with galaxies classified in a completely automatic process, and without human intervention, guaranteeing that the results are not driven by a bias in the human perception.

The results show a statistically significant higher number of galaxies with clockwise handedness compared to galaxies with counterclockwise handedness in the SDSS database. These results are in agreement with previous studies using manually classified galaxies (Shamir 2016, 2012; Hoehn & Shamir 2014), but other studies using a smaller number of galaxies (Shamir 2016) or manually classified galaxies (Land et al. 2008) do not show statistically significant preference for a certain handedness. The differences between some of the measurements are statistically significant, and were deduced using a fully automatic process, leading to the conclusion that the SDSS photometric pipeline is sensitive to the handedness of the galaxy, and provided different photometric measurements for galaxies of different handedness.

Reasons for the asymmetry of the position angle can be the way the position angle is measured. Unlike elliptical galaxies, the morphology of a spiral galaxy can be asymmetric along the major axis, and that asymmetry can be also dependent on the handedness, leading to an error in the measurement of the position angle.

Table 5. MPA-JHU variables measured from clockwise and counterclockwise galaxies.

Variable	Mean clockwise	Mean counterclockwise	t-test P	Bonferroni-corrected t-test P
theta_5	-0.26 ± 0.25	-0.8 ± 0.26	0.13	1
theta_6	0.72 ± 0.41	1.58 ± 0.44	0.15	1
velDispChi2	1922.84 ± 3.03	1930.39 ± 3.26	0.09	1
fracNSigma_8	0.00041 ± 0.00001	0.00044 ± 0.00002	0.16	1
fracNSigma_9	0.0003 ± 0.00001	0.0003 ± 0.00001	0.14	1
fracNSigma_10	0.0002 ± 0.00001	0.0002 ± 0.00001	0.13	1
fracNSigma_8	0.00041 ± 0.00001	0.00044 ± 0.00001	0.16	1
fracNSigma_9	0.0003 ± 0.00001	0.00033 ± 0.00001	0.14	1
fracNSigma_10	0.00023 ± 0.00001	0.00026 ± 0.00001	0.13	1
fracNSigLo_7	0.00017 ± 0.00001	0.00019 ± 0.00001	0.09	1
fracNSigLo_8	0.00011 ± 0.000004	0.00012 ± 0.000004	0.09	1
fracNSigLo_9	0.00017 ± 0.000004	0.00019 ± 0.000004	0.059	1
fracNSigLo_10	0.00005 ± 0.000003	0.000055 ± 0.000004	0.057	1
sn1_i	20.45 ± 0.05	20.64 ± 0.05	0.01	1
sn2_i	21.34 ± 0.05	21.51 ± 0.06	0.035	1
sn1_r	21.75 ± 0.05	21.91 ± 0.06	0.04	1
sn2_r	23.42 ± 0.06	23.57 ± 0.06	0.09	1
sn1_g	20.59 ± 0.05	20.72 ± 0.06	0.1	1
sn2_g	22.72 ± 0.06	22.84 ± 0.06	0.18	1

The mean magnitude of clockwise SDSS galaxies in a certain part of the sky is expected to be approximately the same as the mean magnitude of counterclockwise SDSS galaxies in the same sky region. Therefore, even if the measurements of the magnitude change in different sky regions due to atmospheric or other effects, the measurements should be on average the same for clockwise and counterclockwise galaxies, as all galaxies are in the same sky region. Figure 3 shows the difference between the mean deVMag of galaxies with clockwise handedness and the mean deVMag of galaxies with counterclockwise handedness in different RA sectors of 30°. The graph shows that the difference is smaller around the RA range of (30°, 60°), increases until peaking in the RA range of (180°, 210°), and then starting to decrease. The graph shows a symmetric pattern centred at around the RA range of (180°, 210°).

The inverse Pearson correlation between the cosine of the RA and the measured difference between the g magnitude of clockwise galaxies and g magnitude of counterclockwise galaxies is ~0.868. Given that the sample size is 12, the two-tailed probability to have such correlation by chance is ($P < 0.00025$). Clearly, the other bands are strongly correlated with the g band, and therefore it is expected that all bands exhibit a strong correlation with the cosine of the RA. The Pearson correlation of the u, r, i, and z bands with the cosine of the RA is 0.75, 0.731, 0.787, and 0.761, respectively. The two-tailed probability for having such correlation by chance is 0.005, 0.007, 0.002, and 0.004, respectively.

These results were compared to the differences in the magnitude of clockwise and counterclockwise galaxies in the two smaller datasets used in Shamir (2016). Figure 4 shows the difference between the deVMag of clockwise galaxies and the deVMag of counterclockwise galaxies in different RA
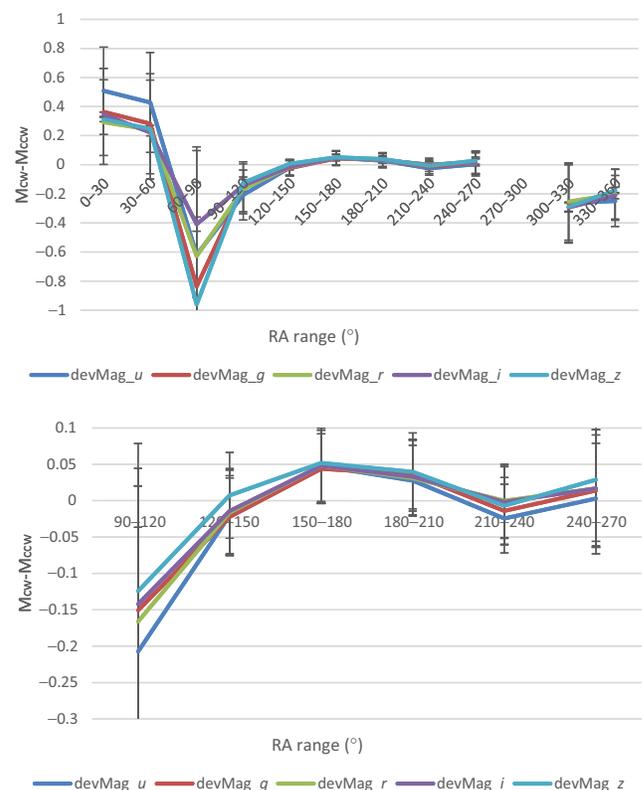

Figure 4. Differences between the de Vaucouleurs magnitude of clockwise galaxies and the de Vaucouleurs magnitude of counterclockwise galaxies in different RA ranges in the u, g, r, i, and z bands. The galaxies are taken from the dataset of automatically classified galaxies used in Shamir (2016). The bottom graph shows just the RA range of (90°, 270°), where the population of the galaxies is higher and therefore the standard error is lower.
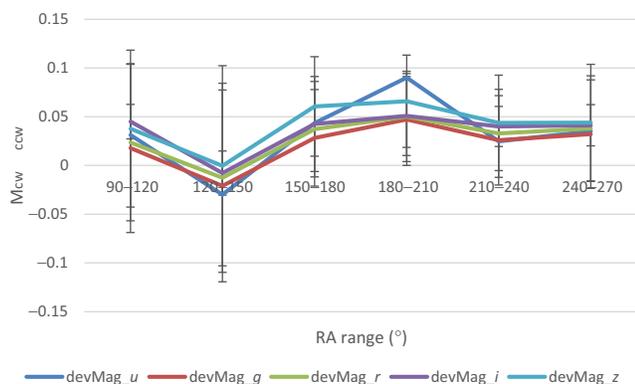
Figure 5. Differences between the de Vaucouleurs magnitude of clockwise galaxies and the de Vaucouleurs magnitude of counterclockwise galaxies in different RA ranges in the *u*, *g*, *r*, *i*, and *z* bands. The galaxies are taken from the dataset of Galaxzy Zoo 2 galaxies used in Shamir (2016). The graph shows the RA range of (90°, 270°), as the galaxies of that dataset are within that RA range.

ranges using the dataset of automatically annotated galaxies used in Shamir (2016). Outside the RA range of (90°, 270°), the population of galaxies is low, making the asymmetry large in some of these weakly populated RA ranges, and therefore the figure shows the differences in the RA range of (90°, 270°).

As the figure shows, within the RA range of (90°, 270°), the dataset used in Shamir (2016) and the dataset used in this paper are largely in agreement. A noticeable exception is the *i* and *z* bands in the (90°, 120°) RA range, but that range also has a larger standard error.

Figure 5 shows the same using the dataset of Galaxy Zoo 2 galaxies used in Shamir (2016). The galaxies of that dataset are within the RA range of (90°, 270°). The differences between the clockwise and counterclockwise galaxies in the Galaxy Zoo 2 dataset are also largely aligned with the results of the dataset used in this study.

The handedness of a spiral galaxy is a crude binary descriptor, and there is no known atmospheric or other effect that can make a galaxy with clockwise handedness seem to have counterclockwise patterns. Also, the ratio between the frequency of clockwise and counterclockwise galaxies is different in different parts of the sky covered by SDSS, and therefore if such asymmetry exists, it is sensitive to the region of the sky. The vast majority of the galaxies used in this study do not have spectra, making it difficult to separate gravitationally interacting superstructures such as the Sloan Great Wall (Gott III et al. 2005).

Measurements of the differences between the magnitude of clockwise and counterclockwise galaxies are taken using galaxies imaged in the same parts of the sky, but are separated by their handedness. The fact that the galaxies are imaged at the same sky region guarantees that the differences are not driven by different atmospheric effects.

Reasons for such asymmetry in the SDSS database could be related to a systematic measurement bias in the photom-

etry pipeline. Related observations have also been related to large-scale asymmetry in the local universe (Longo 2011; Shamir 2012; Gullu & Tekin 2013). While that explanation conflicts with some current cosmological assumptions, current cosmological models might not be complete (Kroupa 2012; Kragh 2013), and the cosmological principle is challenged by the observation of possible large structures (Clowes et al. 2013; Horvath, Hakkila, & Bagoly 2013), exceeding the size limit of structures that do not violate the homogeneity aspect of the cosmological principle (Yadav, Bagla, & Khandai 2010). The observed asymmetry can also be the result of local galaxy properties such as internal extinction along the galaxy arms, which can be linked to the radial velocity. The results described in this study propose questions for further investigation into the source and cause of the observed asymmetry.

The primary downside of the results described in this paper is that they rely on a single source, which is the Sloan Digital Sky Survey. While it is difficult to identify reasons that can cause such asymmetry, photometric pipelines and imaging systems are complex, and can be vulnerable to errors of kinds that have not been identified in the past. Further studies will use equivalent databases such as PanStarrs, as well as far larger databases such as the future LSST to test whether the observation is consistent across databases, or specific to the widely used SDSS database.

ACKNOWLEDGEMENTS

REFERENCES

Abazajian, K. N., et al. 2009, ApJS, 182, 543
Aihara, H., et al. 2011, ApJS, 193, 29
Breiman, L. 1996, Machine Learning, 24, 123
Breiman, L. 2001, Machine Learning, 45, 5
Brinchmann, J., Charlot, S., White, S., Tremonti, C., Kauffmann, G., Heckman, T., & Brinkmann, J. 2004, MNRAS, 351, 1151
Brosche, P. 1973, A&A, 23, 259
Clowes, R. G., Harris, K. A., Raghunathan, S., Campusano, L. E., Söchting, I. K., & Graham, M. J. 2013, MNRAS, 429, 2910
Djorgovski, S., & Davis, M. 1987, AJ, 313, 59
Dong, L., Frank, E., & Kramer, S. 2005, Lecture Notes in Computer Science, 3721, 84
Frank, E., Hall, M., Trigg, L., Holmes, G., & Witten, I. H. 2004, Bioinformatics, 20, 2479
Goeman, J. J., & Solari, A. 2014, Statistics in Medicine, 33, 1946
Gott III, J. R., et al. 2005, ApJ, 624, 463
Gullu, I., & Tekin, B. 2014, PhLB, 728, 268
Hall, M., Frank, E., Holmes, G., Pfahringer, B., Reutemann, P., & Witten, I. H. 2009, ACM SIGKDD Explorations Newsletter, 11, 10
Hoehn, C., & Shamir, L. 2014, AN, 335, 189
Horvath, I., Hakkila, J., & Bagoly, Z. 2013, preprint, arXiv:1311.1104

Kohavi, R. 1995, Lecture Notes in Artificial Intelligence, 912, 174

Kragh, H. 2013, Perspectives on Science, 21, 325

Kroupa, P. 2012, PASA, 29, 395

Kuminski, E., & Shamir, L. 2016, ApJS, 223, 20

Kuminski, E., George, J., Wallin, J., & Shamir, L. 2014, PASP, 126, 959

Land, K., et al. 2008, MNRAS, 388, 1686

Lintott, C., et al. 2011, MNRAS, 410, 166

Longo, M. J. 2011, PhLB, 699, 224

Shamir, L. 2009, MNRAS, 399, 1367

Shamir, L. 2011a, The Astrophysics Source Code Library, p. ascl:1105.011

Shamir, L. 2011b, ApJ, 736, 141

Shamir, L. 2012, PhLB, 715, 25

Shamir, L. 2016, ApJ, 83, 32

Shamir, L., Orlov, N., Eckley, D. M., Macura, T., Johnston, J., & Goldberg, I. G. 2008, Source Code for Biology and Medicine, 3, 13

Shamir, L., Orlov, N., Eckley, D. M., Macura, T., Johnston, J., & Goldberg, I. 2013, Astrophysics Source Code Library, p. ascl:1312.002

Willett, K. W., et al. 2013, MNRAS, 435, 85

Yadav, J. K., Bagla, J., & Khandai, N. 2010, MNRAS, 405, 2009

York, D. G., et al. 2000, AJ, 120, 1579

Appendix: Sample dataset of 800 galaxies

The following Figures A1 and A2 show the 400 sample clockwise galaxies and 400 sample counterclockwise galaxies, respectively.
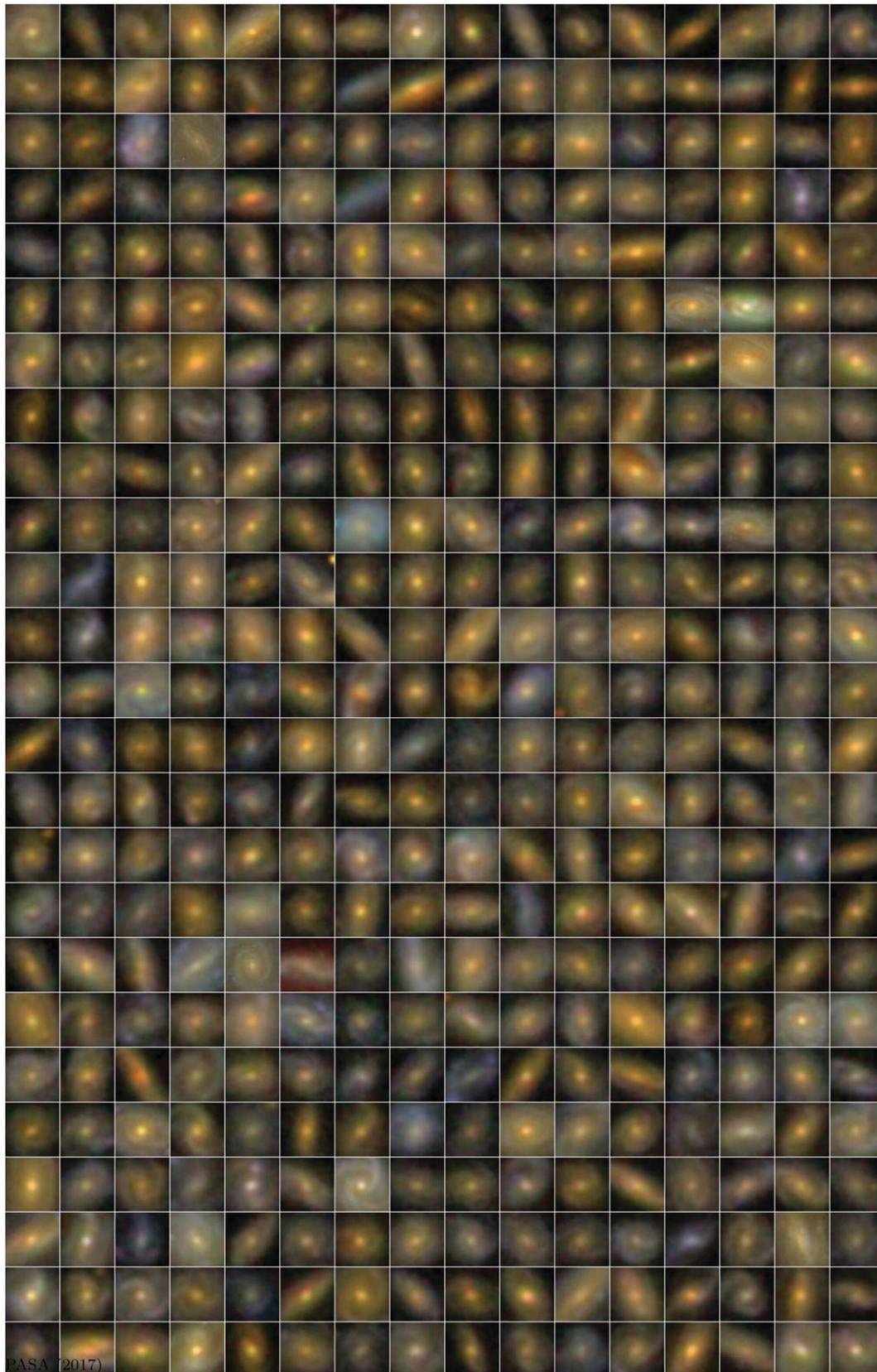
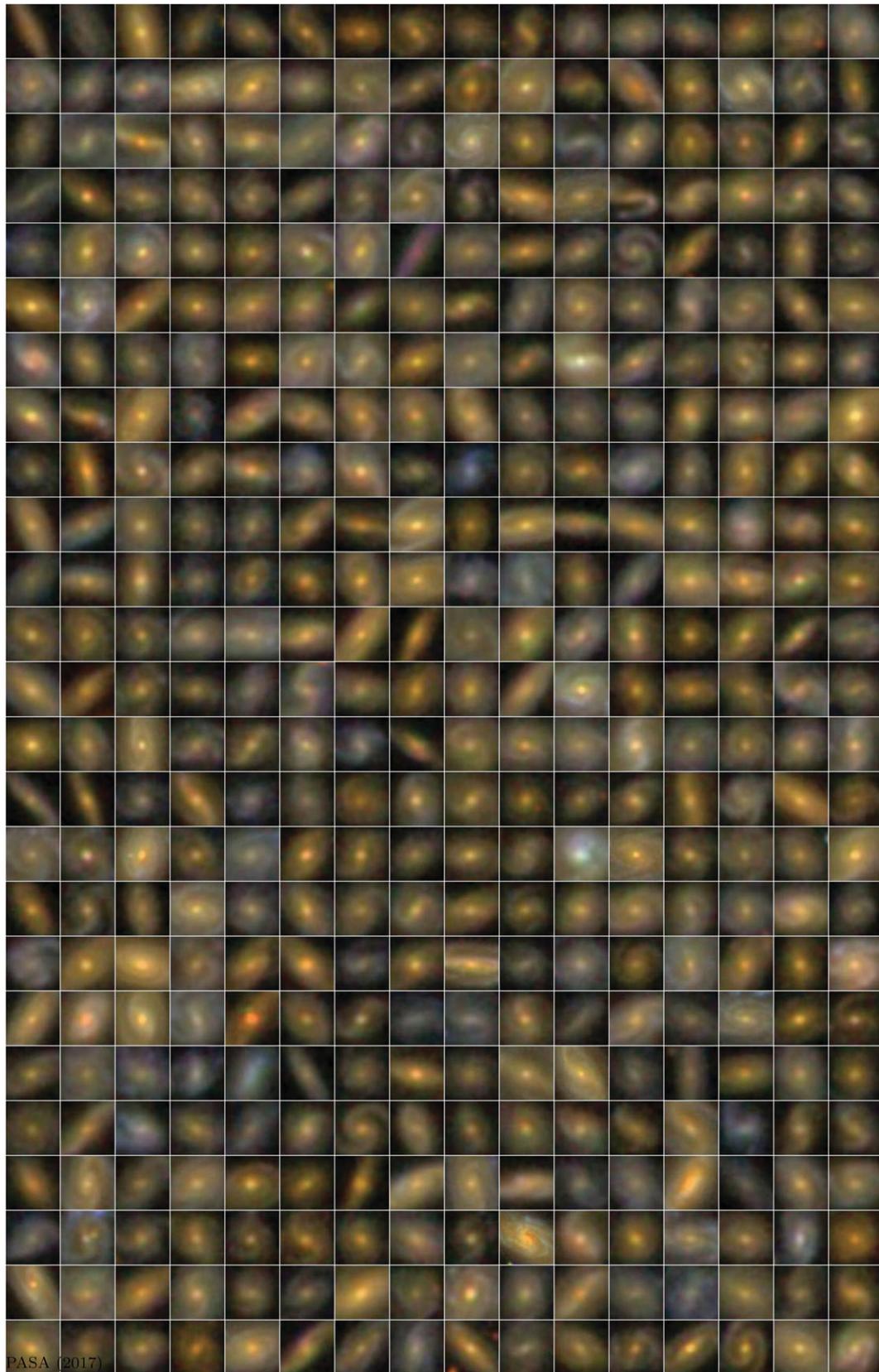**Figure A1.** The sample dataset of 400 galaxies with clockwise handedness.

Figure A2. The sample dataset of 400 galaxies with counterclockwise handedness.